

Nabholz, Stoll, and Waffler⁵ have investigated the energy distribution of α -particles ejected from heavy nuclei in photographic emulsions by lithium γ -rays. They estimate that the contribution of silver to the spectrum at its peak is negligible but find close agreement between the observed spectrum and that calculated from statistical theory for bromine. Accordingly they calculate the average $\text{Br}^{79,81}(\gamma, \alpha)$ cross section at 17.6 Mev to be $(1.2 \pm 0.5) \times 10^{-28} \text{ cm}^2$. For Br^{81} at this energy we find the cross section to be $0.80 \times 10^{-28} \text{ cm}^2$. Making the same assumptions as Nabholz *et al.* regarding the cross-section ratios for the two isotopes we obtain $1.3 \times 10^{-28} \text{ cm}^2$ as the average cross section for bromine at 17.6 Mev, in agreement with the above value.

It might be noted that the small number of α -particles with energies higher than the theoretical spectrum for bromine in Fig. 1 of reference 5 might arise from silver and would in no way affect the good agreement noted above.

Haslam, Cameron, Cooke, and Crosby⁶ made no attempt to separate the effects of silver and bromine since their observed α -spectrum did not agree closely with theoretical distributions for either element. The methods described in their paper, while suitable for investigation of the general features of photo-alpha processes, are not well adapted to accurate determination of cross sections at a particular energy. Statistics in photographic emulsion work are poor, and the effect is aggravated by the use of a continuous rather than a discrete photon spectrum. If silver is assumed to make a negligible contribution at 17.6-Mev excitation, a cross section of $3 \times 10^{-28} \text{ cm}^2$ for an average bromine nucleus is obtained, but this value is open to considerable doubt due to the steepness of the cross-section curve in this energy region.

We wish to thank Dr. K. J. McCallum of the Department of Chemistry for helpful advice and Mr. L. H. Greenberg for valuable discussions. This work was supported by the National Research Council of Canada.

¹ L. Katz and A. G. W. Cameron, *Can. J. Phys.* **29**, 518 (1951).

² Haslam, Smith, and Taylor, *Phys. Rev.* **84**, 840 (1951).

³ R. N. H. Haslam and H. M. Skarsgard, *Phys. Rev.* **81**, 479 (1951).

⁴ A. K. Mann and J. Halpern, *Phys. Rev.* **82**, 733 (1951).

⁵ Nabholz, Stoll, and Waffler, *Phys. Rev.* **86**, 1043 (1952).

⁶ Haslam, Cameron, Cooke, and Crosby, *Can. J. Phys.* (to be published).

⁷ C. H. Millar and A. G. W. Cameron, *Can. J. Phys.* (to be published).

The Angular Distribution of Fission Fragments in the Photofission of Thorium*

E. J. WINHOLD, P. T. DEMOS, AND I. HALPERN

Physics Department and Laboratory for Nuclear Science, Massachusetts Institute of Technology, Cambridge, Massachusetts

(Received July 28, 1952)

MEASUREMENTS of the angular distribution of photofission fragments from thorium have been made using the x-ray beam of the MIT linear accelerator. They were performed by counting the β -activities of the fragments which were emitted from a thorium foil and caught at various angles to the x-ray beam. The observed angular distribution has a maximum at right angles to the beam and the amount of the anisotropy decreases with increasing photon energy.

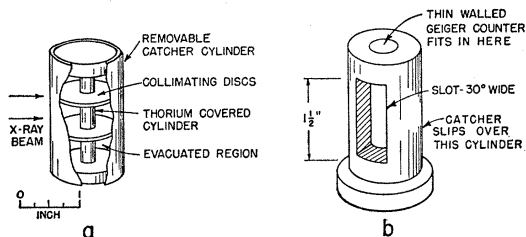


FIG. 1. The arrangements for exposure and counting of the cylindrical fragment catcher. After exposure the catcher is slipped over the cylinder in *b* and rotated so as to expose (to the counter inside) the activities caught at various angles to the x-ray beam.

With the accelerator running at about 16 Mev, the set-up shown in Fig. 1(a) was exposed at 6 inches from the x-ray target. It consists essentially of two concentric cylinders; the inner one is covered with thorium foil which is thick to fission fragments and the outer one serves as the fragment catcher. The activities of 30°-wide strips of this catcher cylinder (each strip corresponding to a different angle of fragment emission with respect to the beam) are measured after the exposure by means of the arrangement of Fig. 1(b).

A number of runs have been made at 16 Mev with this arrangement, and the results are given in the following table normalized

θ	0°	45°	90°	135°	180°	270°
Measured activity for slot 30° wide	1.00	1.14 ± 0.06	1.34 ± 0.03	1.22 ± 0.07	1.00 ± 0.06	1.31 ± 0.07

to the activity at 0° with respect to the x-ray beam. It is seen that the distribution is peaked at 90° and is symmetrical from front to back. These facts and the amount of activity measured at 45° and 135° suggest that the angular distribution can be written in the form $a + b \sin^2\theta$. When the data in the table is corrected for the

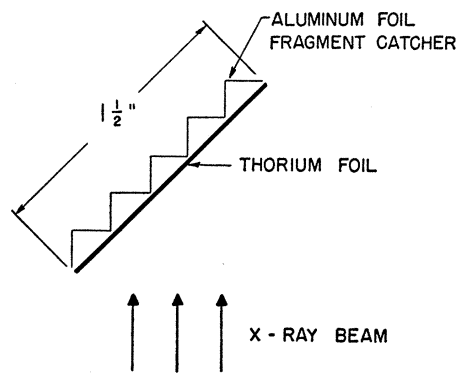


FIG. 2. The exposure geometry used in the energy-dependence runs.

finite angular resolution of the exposure and counting arrangements,¹ the ratio b/a is 0.41 ± 0.09 . Some small corrections have been made for x-ray flux variations over the target, and it was established that a negligible fraction of the observed fissions are caused by fast neutrons.

It is conceivable that the measured asymmetry might involve not only different numbers of fragments at 90° and 0°, but also different types of fragments. To check this possibility, the exposure time in the experiment was varied. No dependence of the angular asymmetry on exposure times (from 6 minutes to 3 hours) or on the counting time was found. This would seem to imply that the same fragments are emitted in all directions. The question of a possible connection between the angular distribution and the fragment mass distribution is being investigated more carefully at the present time by means of a technique involving chemical separations.

In order to examine the energy dependence of the angular distribution it was necessary to use the arrangement of Fig. 2. This arrangement sacrifices angular resolution in order to keep the intensity up at the lower energies, where the photofission yield is small. A sheet of one-mil aluminum foil folded into a step-like shape serves as the fragment catcher; it is exposed next to a thorium foil set at 45° to the x-ray beam. Thus alternate faces receive fragments emitted mainly at 90° and 0° to the beam. After exposure the foil is flattened out and counted under a brass mask covering either set of faces. Checks were made to show that flux non-uniformities and the counting geometry introduced no serious errors in the results.

The geometrical corrections for angular resolution are necessarily rather large in this arrangement. At 16 Mev the measured activity ratio was 1.09 ± 0.03 for the 90° faces to the 0° faces. This

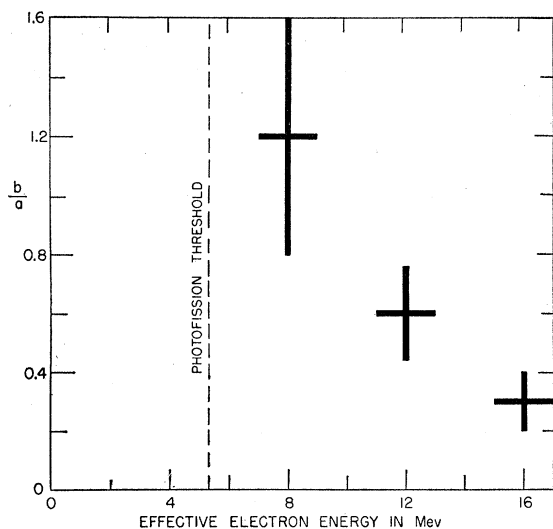


FIG. 3. The dependence of the asymmetry b/a as a function of effective electron energy for an angular distribution of the form $a + b \sin^2\theta$.

corresponds to a value for b/a of 0.30 ± 0.10 , agreeing with the cylinder results within the errors of the two experiments.

A number of runs using the step-like geometry were made at energies from about 8 to 16 Mev. The asymmetry was found to increase rapidly as the accelerator energy was decreased (Fig. 3). Unfortunately the electron spectrum is about 3 Mev wide and it has not been possible to determine the "effective energy" of the electrons to better than about 1 Mev. This energy uncertainty and the use of a thick x-ray target prevent us at present from being able to give b/a as a function of photon energy.

No really convincing explanation of the observed angular distribution has so far been developed. The form of the distribution suggests an electric dipole transition, but the ratio of e/m values for the fission end products does not indicate a process involving a particularly large dipole moment. The energy dependence shows, moreover, that the effect is not largest at the dipole resonance peak in thorium (~ 15 Mev). This may, however, not be particularly significant because most fissions caused by 15-Mev photons may come from (γ, n_f) reactions rather than (γ, f) reactions and the former would perhaps be expected to give a more isotropic fragment distribution. If very strong selection rules obtain for the allowed spins of the fragments at the moment of fission, the angular momentum brought in by the photon might on the average go mostly to the orbital momentum between the fragments. Although this would "explain" an angular distribution, it involves a rather arbitrary assumption. In order to investigate any dependence of the angular distribution on spins, we are preparing to repeat the experiment with a number of other fissionable materials having various ground-state spins.

* This research has been supported by the joint program of the ONR and AEC. A preliminary report appears in Phys. Rev. **85**, 728 (1952).

¹ In this geometrical correction, it is assumed that fragments emitted isotropically would emerge from a thick foil in a cosine distribution with respect to the foil normal. This has been checked experimentally to about 10 percent.

The Beta-Spectrum of $\text{He}^{6\ddagger}$

C. S. WU, B. M. RUSTAD, V. PEREZ-MENDEZ, AND L. LIDOFKY
Columbia University, New York, New York
(Received August 5, 1952)

THE beta-spectrum of He^6 is of great theoretical interest. Not only can its linear Kurie plot serve to exclude one of the Fierz interference terms (A , T), but its end point together with its half-life determines an ft value which helps to estimate the rela-

tive contributions of the Fermi (S or V) and Gamow-Teller (A or T) interactions in the process of beta-decay.

The only reported measurement of the He^6 beta-spectrum was made on a semicircular focusing magnetic spectrometer and gave an end point of 3.215 Mev.¹ This end point together with $t_{1/2} = 0.823 \pm 0.013$ sec² yields an ft value of 584 sec.

Because of its theoretical interest we have recently remeasured the beta-spectrum of He^6 using the Columbia magnetic solenoidal spectrometer whose characteristics have been well investigated.

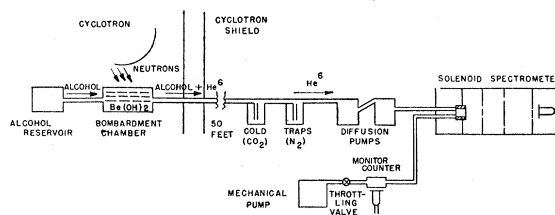


FIG. 1. Block diagram of apparatus.

The spectrometer was placed about 50 feet from the cyclotron to minimize the effects of stray fields from the cyclotron magnet. The spectrometer axis was oriented parallel to the small horizontal component of the nearly vertical stray field, while the vertical component was compensated by a pair of Thomson coils.

The He^6 , produced by the reaction $\text{Be}^9(n, \alpha)\text{He}^6$, was swept from the target chamber with ethyl alcohol vapor. Before reaching the spectrometer source chamber, the alcohol vapor was frozen out in CO_2 and N_2 cold traps and the He^6 concentrated by two successive oil diffusion pumps as shown in Fig. 1.

The source chamber was an aluminum cylinder 1.5 cm diameter by 1 cm depth with a 2-mg/cm² mica front window and a 3-mg/cm² mica back window. After passing through the source chamber, the He^6 entered a monitor counter chamber and was finally evacuated by a mechanical pump.

Data were taken in the following manner to reduce background from the cyclotron. The cyclotron was turned on for 5 sec. A half-

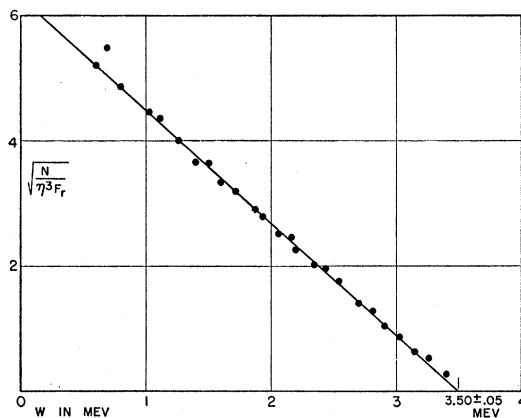


FIG. 2. Kurie plot of He^6 beta-spectrum.

second later, the spectrometer and monitor GM counters were turned on for 5 sec. This cycle was controlled by a system of relays actuated by a cam shaft driven by a synchronous motor. Under these conditions the radioactive purity of the source was > 98 percent.

The baffle slit in the spectrometer together with the source volume used gave 5-6 percent resolution. The Kurie plot shown in Fig. 2 is linear from its end point of 3.50 ± 0.05 Mev to about 0.6 Mev, below which counting statistics became very poor. The end point together with $t_{1/2} = 0.823$ yields the ft value of He^6 of 815 ± 70 sec.³ Moszkowski⁴ estimated the relative contribution of